

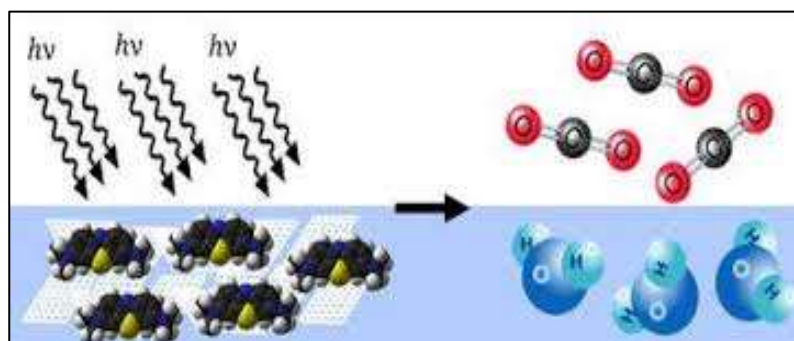
15. Photocatalysis for Waste Water Treatment

**Rakshit Ameta, Lalita Joshi,
Deepika Patel, Jyotsana Panwar,
Suresh C. Ameta**

Department of Chemistry,
PACIFIC University, Udaipur, Rajasthan.

S. Ravichandran

Department of Chemistry,
School of Mechanical Engineering,
Lovely Professional University,
Jalandhar, Punjab.



Abstract:

Water is an important constituent of life support system. No life can survive and no one can even dream to live without water. The majority of water resources are polluted becomes of fast industrial growth, urbanization and anthropogenic problems due to rapid growth in population. Out of these, main sources of water pollution are industrial effluents, agricultural discharges, sewage and other wastes. These effluents are responsible for posing a larger problem of water pollution so that water remains no longer suitable for drinking and agriculture purposes. It has been reported that more than 2.6 billion people (about 2/5th of world's population) still lack basic sanitation facilities. As a consequence, more than 10% people are still having drinking water sources, which are not safe.

15.1 Introduction:

Water is one of the most important natural resources for human kind. Water pollution is one of the major problems faced by the humans. Microbial and chemical contaminations challenges are there before the world in providing safe and clean water to the society. Organic pollutants in industrial and agricultural sewage are a serious threat to the environments as well as human health. Major water pollutants are represented in Figure 15.1

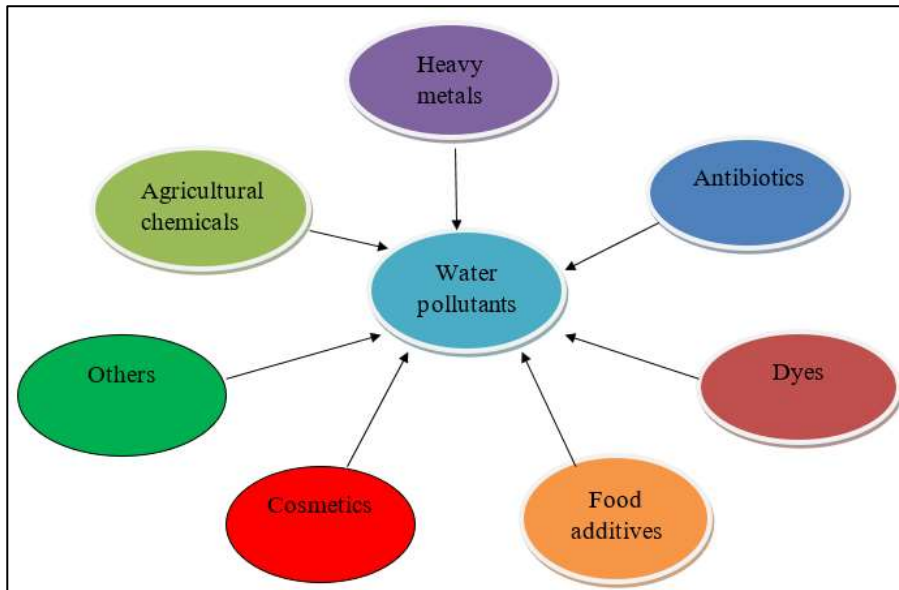


Figure 15.1: Major Water Pollutants

They produce a major problem of water pollution. Because of water pollution, thousands of children die every day from different waterborne diseases such as diarrhea, cholera, typhoid etc. The adverse effects of water pollution still remained a major source of causing health problems. These are represented in Figure 15.2

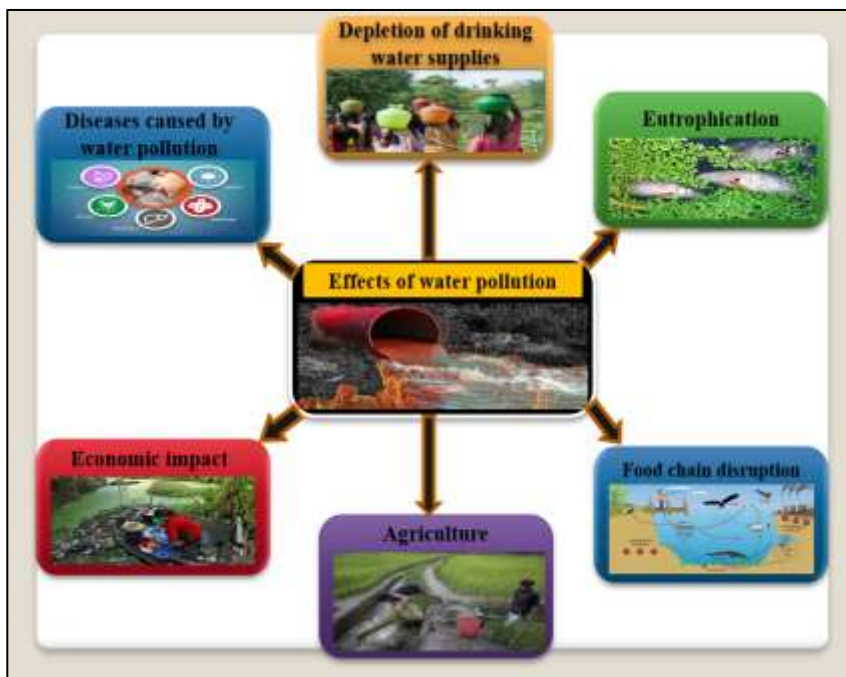


Figure 15.2: Adverse Effects of Water Pollution

Some of these known techniques used for water and wastewater treatment are:

- Electrodeposition,
- Electrocoagulation,
- Electro flotation,
- Electrooxidation,
- Screening, aeration and pre-chlorination,
- Filtration,
- Settling or sedimentation,
- Coagulation and flocculation,
- Disinfection and chlorination,
- Aeration,
- Biofiltration, and
- Oxidation ponds.

Various wastewater treatment technologies are available, which are different from each other in regards to their principles, economy, application, and speed. Common methods of wastewater treatment are classified as biological, chemical and physical treatments.

Many methods of treatment of pollution water have been suggested and used for last few decades. But all these methods are associated with some or the other disadvantage. Therefore, there is a need for fast, low cost, effective and green chemical technology and search is still on. Advanced oxidation process (AOPs) are significantly efficient for complete destruction of pollutants like, naturally occurring toxins, pesticides, dyes, phenols, EDS, etc. AOPs have been proposed to degrade even recalcitrant molecules. Advanced oxidation process is a wastewater treatment process, which is used to convert polluted water into useful form with relatively less or negligible health and environment issues. Treated waste water is then returned back to water-cycle and it can be reused.

15.2 Advanced Oxidation Processes (AOPs):

Advanced oxidation processes in a broad sense, refer to a set of chemical treatment procedures designed to remove organic (and sometimes inorganic) materials in water and waste water by oxidation through reactions with hydroxyl radicals ($\bullet\text{OH}$), holes (h^+), superoxide anion radical ($\text{O}_2^{\bullet-}$), hydroperoxy radical (HO_2^{\bullet}), etc. There are six major types of advanced oxidation processes such as photolysis, photocatalysis, electrochemical oxidation technologies, sonolysis, Fenton-based reactions, and ozone-based processes.

AOPs have several advantages in the field of water treatment:

- They can effectively eliminate organic compounds in aqueous phase, rather than collecting or transferring pollutants into another phase.
- Due to the reactivity of $\bullet\text{OH}$, it reacts with many aqueous pollutants non-selectively without discrimination. AOPs are therefore applicable in many such scenarios if not all, where a number of organic contaminants are to be removed at the same time.
- Some heavy metals can also be removed in forms of $\text{M}(\text{OH})_x$ precipitates.

- Disinfection can also be achieved in some AOPs, which makes these AOPs integrated solution to some water quality problems.
- Since the complete reduction product of $\bullet\text{OH}$ is water and therefore, theoretically speaking AOPs do not introduce any new hazardous materials into the water.
- One of the major advantages of AOPs is transformation or complete mineralization of organic pollutants; even persistent organic pollutants (POPs) to simple stable inorganic compounds such as water, carbon dioxide, and salts with negligible or no sludge production. Hence, it may not require another sludge treatment stage.

15.3 Photocatalysis:

Photocatalysis is a developing branch of chemistry, which deals with chemical reactions proceeding in the presence of light and photocatalyst. Basically, a photocatalyst is a semiconductor, which increases the rate of a reaction in presence of light. There is a wide range of applications of photocatalyst such as water purification, antibacterial, deodorizing, air purifying, antifogging, self-cleaning, etc.

Here, superhydrophilicity played an important role. As it is a green chemical route and therefore, it is the requirement of the day. The term photocatalyst is a combination of two words: photo related to photon and catalyst, which is a substance altering the reaction rate in its presence. Therefore, photocatalysts are materials that change the rate of a chemical reaction on exposure to light. This phenomenon is known as photocatalysis. The substrate that absorbs light and acts as a catalyst for chemical reactions is known as a photocatalyst. All the photocatalysts are basically semiconductors. Photocatalysis is a phenomenon, in which an electron-hole pair is generated on exposure of a semiconducting material to light. Electrons in conduction band can reduce any substrate, while holes in valence band can generate $\bullet\text{OH}$ radical, which is a strong oxidant and it can oxidize many organic compounds. The mechanism of photocatalysis is represented in Figure 15.3

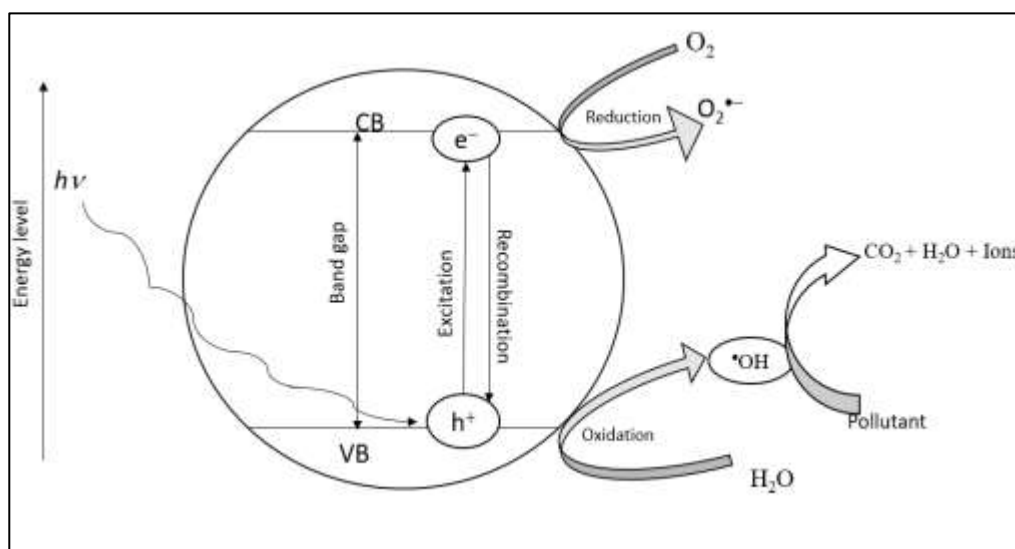


Figure 15.3: Mechanism of Photocatalysis

The photocatalytic reactions can be categorized into two types on the basis of physical state of reactants.

- **Homogeneous photocatalysis:** When both; semiconductor and reactant are in the same phase, i.e. gas, solid, or liquid, such photocatalytic reactions are termed as homogeneous photocatalysis.
- **Heterogeneous photocatalysis:** When both; semiconductor and reactant are in different phases, such photocatalytic reactions are classified as heterogeneous photocatalysis.

Photocatalysts are defined as materials, which decompose detrimental substances under the sun lights containing UV rays. Mainly, TiO₂ and ZnO are used as photocatalyst for a long. Among polymorphs of TiO₂, anatase phase shows the most effective photocatalytic effect. The different methods for photocatalyst preparation include sol-gel, coprecipitation, hydrothermal, solvothermal, sonochemical, chemical vapour deposition, etc. Photocatalysts may be used for antifouling, antifogging, conservation and storage of energy, deodorization, sterilization, self-cleaning, air purification, wastewater treatment, etc.

Modification of Photocatalyst

Efficiency of a photocatalyst can be enhanced by:

- Formation of localized state just above the valence band,
- Formation of localized state just below the conduction band,
- Using photocatalyst with low band gap, and
- Color center formation in band gap and surface modification.

Some of the important techniques for modification of photocatalyst are:

- Doping with metal or nonmetal,
- Codoping with various combination of donor and acceptor materials,
- Coupling of photocatalyst, composite formation,
- Sensitization,
- Use of co-catalyst, and
- Use of heterojunction (Z-scheme and S- scheme).

15.4 Photocatalytic Degradations:

Photocatalytic degradation is an advanced oxidation process, which can be used to degrade pollutants with high concentration, complexity and low biodegradability. Photocatalytic degradation uses light energy to drive degradation of pollutant.

Ledakowicz et al.¹ investigated treatment of synthetic wastewater and simulating effluents from knitting industry using AOPs. The wastewater contained an anionic detergent (Awiważ KG), a softening agent (Tetrapol CLB) and acid blue 40 (AB₄₀). It was reported that AB₄₀ did not undergo biodegradation without AOPs pretreatment.

They studied the effects of various oxidants like H_2O_2 and O_3 in presence of UV light on biodegradation of textile water. Tang et al.² investigated photocatalytic degradation of methylene blue (MB) over CaIn_2O_4 photocatalyst under visible light irradiation in 2 h at room temperature. It was reported that high activity could be retained in a wide range of wavelength even up to 580 nm. The SO_4^{2-} ions were detected as a product of degradation of MB, indicating that this dye was completely mineralized in this process.

Liqiang et al.³ modified ZnO nanoparticles photocatalysts by depositing Pd on their surfaces via photoreduction method. It was observed that content of crystal lattice oxygen decreased on surface of ZnO nanoparticles, when sufficient amount of Pd was deposited, but adsorbed oxygen increased, which indicated that Pd was deposited on the crystal lattice oxygen. As a result, the activity of ZnO nanoparticles was significantly improved in gas phase photocatalytic oxidation of $n\text{-C}_7\text{H}_{16}$. It was concluded that photocatalytic activity of Pd-deposited ZnO nanoparticles was higher.

Chen et al.⁴ prepared a visible light active TiO_2 photocatalyst via surface chemical modification using toluene 2,4-diisocyanate (TDI). It was reported that as-prepared TiO_2 -TDI had absorption in the visible region due to LMCT excitation of the surface complex. This TiO_2 -TDI photocatalyst had a good photostability and it also exhibited high photocatalytic performance for the degradation of organic pollutants. It was revealed that turnover number of this photocatalyst for photodegradation of 2,4-dichlorophenol could reach 15.43 after five times reuse of this photocatalyst under visible light irradiation.

Wu et al.⁵ prepared boron and carbon modified visible light-active TiO_2 photocatalyst through sol-gel followed by a solvothermal process. It was reported that as-prepared boron and carbon modified TiO_2 exhibited absorption in visible range (400–500 nm). It was also revealed that there is oxygen vacancy also in samples of carbon and boron modified TiO_2 . It was found that this modified TiO_2 has higher photocatalytic activity on the degradation of acid orange 7 (AO7) in aqueous solution on visible light exposure than carbon modified TiO_2 and undoped anatase TiO_2 .

Pan and Zhu⁶ synthesized BiPO_4 with a nonmetal oxy acid via hydrothermal method. The as-prepared BiPO_4 photocatalyst has a band gap of 3.85 eV. It was found that the photocatalytic activity of BiPO_4 was almost double than that of TiO_2 (P25, Degussa) in degradation of methylene blue (MB), but BET surface area of BiPO_4 is just one tenth of compared to TiO_2 P25.

It was revealed that higher position of the valence band and separation efficiency of electron-hole pairs are responsible for higher photocatalytic activity of BiPO_4 . It was concluded that an inductive effect of PO_4^{3-} helped in separation of e^-/h^+ providing BiPO_4 an excellent photocatalytic activity.

Yu et al.⁷ prepared Fe (III)/AgBr photocatalysts by grafting Fe (III) cocatalyst on surface of AgBr particles via an impregnation method. They evaluated photocatalytic performance by the photocatalytic decolorization of methyl orange solution in presence of visible-light. It was reported that the Fe (III) cluster acted as an effective cocatalyst. It not only improved the photocatalytic activity of AgBr photocatalyst, but it also increased photoinduced

stability of photosensitive AgBr. It was revealed that photocatalytic activity of AgBr photocatalyst surface coated by Fe (III) cocatalyst (8.2 at. %) was enhanced by a factor of 73% and it can be reused even after five cycles.

Bai et al.⁸ prepared C₆₀ modified graphitic carbon nitride composite (C₆₀/g-C₃N₄) via thermal treatment at 550° C, which involved polymerization of dicyandiamide in the presence of C₆₀. It was reported that the valence band (VB) of g-C₃N₄ shifted to a lower energy state, when C₆₀ was incorporated into the matrix of g-C₃N₄. It provides strong photo-oxidation capability to as-prepared composite under visible light. This composite exhibited enhanced degradation of methylene blue (MB) and phenol in presence of visible light ($\lambda > 420$ nm). The C₆₀/g-C₃N₄ composites had high photocatalytic degradation activities as compared to bulk g-C₃N₄. This enhanced photocatalytic activity may be due to holes and •OH radicals. It may be attributed to strong interaction of conjugative π -bond between g-C₃N₄ and C₆₀.

The ZnO nanoneedles (ZNNs) were grown by Tripathy et al.⁹ in large quantity by thermal evaporation approach on non-catalytic silicon substrates. It was then used as effective photocatalyst for photocatalytic degradation of methyl orange (MO). It was observed that as-synthesized nanostructures were having high density and exhibited high-crystallinity with good optical properties. The photocatalytic properties of ZNNs were investigated under UV light irradiation. It was also revealed that degradation rate of ~95.4% of MO could be achieved within 140 min. Balcha et al.¹⁰ synthesized zinc oxide nanoparticles via precipitation and sol-gel methods. It was revealed that their hexagonal wurtzite structure with crystallite sizes of 30 and 28 nm were obtained, respectively. The photocatalytic activities of as-prepared samples were evaluated by photocatalytic degradation of methylene blue under UV radiation. It was also revealed that (20 to 100 mg L⁻¹) 81.0 and 92.5 % dye could be degraded on using ZnO (250 mg L⁻¹) prepared by precipitation and sol-gel methods, respectively. It was concluded that sol-gel method can be preferred over precipitation method.

Thi and Lee¹¹ prepared visible light-driven photocatalysts of lanthanum (La) doped ZnO nanoparticles via precipitation method using different La doping concentrations (0.5, 1.0 and 1.5 wt%). It was reported that although La doping did not affect the crystallinity of ZnO much more, but it increased optical absorption of visible light due to the reduction in band gap energy and particle size. The La-doped ZnO photocatalyst was then used for treatment of paracetamol (100 mg L⁻¹) in aqueous solution for 3 h under visible light irradiation. It was revealed that 1.0 wt% La-doped ZnO photocatalyst exhibited highest photocatalytic activity in degrading paracetamol and it could achieve a degradation efficiency of 99% and TOC removal of 85%.

Sudrajat and Babel¹² synthesized N-doped ZnO (N-ZnO) via combustion route. The photocatalytic activity of N-ZnO was evaluated for degradation of amaranth (AM) and methylene blue under visible and UV light. It was reported that N-doping extended the spectral response in visible region and even up to the near-infrared region using 1 g L⁻¹ of N-ZnO at pH 7. It was also revealed that 89.3% of methylene blue (10 mg L⁻¹) could be degraded within 1.5 h under visible light, while 4 h are required with N-ZnO and it can degrade only 88.5% of amaranth.

Wu et al.¹³ constructed a composite of *p*-type LaFeO₃ microspheres coated with *n*-type nanosized graphitic carbon nitride nanosheets (g-C₃N₄). It was reported that as-prepared LaFeO₃/g-C₃N₄ *p-n* heterostructured photocatalyst exhibited enhanced visible-light absorption, efficient and effective separation and migration of charge carriers. As a result, this composite displayed higher visible-light photocatalytic activity for the degradation of brilliant blue, which was 7.8 and 16.9 times than that of LaFeO₃ and pristine g-C₃N₄, respectively. The photogenerated holes, superoxide radicals and hydroxyl radicals played active role as oxidants in this degradation process. Z-scheme charge carrier transfer pathway has been proposed to explain this dye-sensitization effect.

Huang et al.¹⁴ prepared molybdenum disulfide (MoS₂) microspheres and used them as a photocatalyst for the degradation of thiobencarb (TBC) in presence of visible-light. It was reported that degradation efficiency could reach to 95% in 12 h in the pH range of 6–9. The effect of presence of some anions (Cl⁻ and NO₃⁻) was negligible on the photocatalytic activity of MoS₂. It was predicted that hydroxyl radicals and holes played the role of reactive species in this process as indicated by scavengers' studies. The practicality of as-prepared MoS₂ photocatalyst was confirmed by using it in the removal of TBC from real water samples. Its stability and reusability were also ascertained in three successive runs.

Jiang et al.¹⁵ fabricated hexagonal boron nitride (h-BN) decorated g-C₃N₄ metal-free heterojunction so that surface area is more and charge separation is also promoted. The photocatalytic activity of as-prepared h-BN/g-C₃N₄ composites was evaluated in degradation of rhodamine B and tetracycline under visible light irradiation. It was observed that h-BN/g-C₃N₄ composites exhibited much higher photocatalytic activity as compared to g-C₃N₄ and h-BN. It was reported that photocatalytic efficiency of BC-3 sample was 2.3 and 60.3 times higher in degrading TC than its individual components g-C₃N₄ and h-BN, respectively. Similarly, it was also 7.3 and 11.8 times higher than g-C₃N₄ and h-BN for RhB degradation, respectively. This enhanced photocatalytic activity of h-BN/g-C₃N₄ composite was attributed to increase in surface area and h-BN nanosheet, which acted as promoter for photoexcited holes transfer.

Lu et al.¹⁶ synthesized type II ZnIn₂S₄/BiPO₄ heterojunction via hydrothermal route. The morphology of as-prepared composite was dandelion-like microflower heterostructure. It was observed that the highest photocatalytic activity was there on using 70 wt% ZnIn₂S₄/BiPO₄ heterojunction, which can degrade about 84% tetracycline (40 mg L⁻¹) in 90 min. This activity was about 1.89 and 3.14 times higher as compared to ZnIn₂S₄ and BiPO₄, respectively. Improved separation efficiency of electron-hole pairs was mainly attributed due to type II heterojunction between ZnIn₂S₄ and BiPO₄, during the photocatalytic reaction. It was confirmed that •OH and O₂^{•-} were active oxidizing species in this photocatalytic system. Mahanthappa et al.¹⁷ synthesized CuS, CdS and CuS-CdS nanocomposite photocatalysts via hydrothermal method. They also evaluated as-prepared materials for degradation of methylene blue in the presence of hydrogen peroxide (as an oxidant) under visible light irradiation. It was also revealed that about 80, 59 and 99.97% MB dye (10 ppm) degraded by could be degraded using for CuS, CdS and CuS-CdS nanocomposite, respectively in 10 min. This higher activity of CuS-CdS nanocomposite was attributed to narrow band gap, large surface area, low recombination of the photo-generated electrons and holes and high adsorbing capacity of the dye.

Tichapondwa et al.¹⁸ investigated photocatalytic degradation of methylene blue over three commercial TiO₂ powders as catalysts having different crystal phases. Degradation studies were then conducted on 10 ppm MB solutions using these three powders. It was found that Degussa P25 TiO₂, (mixture of rutile and anatase) was the most efficient as compared to the neat anatase and rutile powders and it could degrade 81.4% of the MB. About 95% degradation was achieved on using 0.5 g L⁻¹ catalyst loading at pH 10. It was revealed that doping with copper increased degradation by 2% but zinc doping reduced it to 90%.

Kiwaan et al.¹⁹ synthesized titanium dioxide photocatalyst via low temperature co-precipitation process and used for photocatalytic degradation of rhodamine B and acid red 57 (AR57) under UV irradiation. It was observed that the sample annealed at 400°C exhibited highest photocatalytic dye degradation efficiency of 93.8 and 90.7% for RhB and AR57, respectively in 190 min. It was found that degradation of RhB and AR57 involved OH[•] radicals as main oxidizing species.

Tripathi et al.²⁰ reported preparation of fluorescent selenium nanoparticles (SeNPs) using *Ficus benghalensis* leaf extract. It was observed that the size distribution of these SeNPs was found to be in the range of 45–95 nm, and the average particle size was 64.03 nm. It was also revealed that as-synthesized SeNPs have been used for the photocatalytic degradation of methylene blue and 57.63% of dye degradation could be achieved in 40 min.

Aziz et al.²¹ prepared chitosan-zinc sulfide nanoparticles (CS-ZnS-NPs). It was observed that their average particle size was 40 nm. The photocatalytic efficiency of as-prepared CS-ZnS-NPs was evaluated for degradation of acid brown 98 and acid black 234 using UV lamp (254 nm). It was reported that at optimal conditions, these NPs could degrade 96.7% acid black 234 in 100 min, while 92.6% for acid brown 98 was removed in 165 min. It was easily recovered and reused for four cycles.

Uheida et al.²² developed a sustainable green photocatalytic technique for removal of microplastics from water using visible light. It was reported that photocatalytic degradation of microplastics, polypropylene (PP) (spherical particles) under visible light irradiation for two weeks of zinc oxide nanorods (ZnO NRs) (immobilized onto glass fibers) resulted in reduction of the average particle volume by 65%. The main photodegradation by-products were identified as mostly nontoxic in nature as evident from GC/MS analysis.

Liu et al.²³ synthesized BiVO₄/Ag₃VO₄ composite via a combination of hydrothermal and chemical deposition process. Then they used it for degradation of methylene blue under visible light. It was revealed that 40%BiVO₄/Ag₃VO₄ composite exhibited excellent photocatalytic degradation properties with rate constant 0.05588 min⁻¹, which was about 1.76 and 22.76 times than that of Ag₃VO₄ (0.03167 min⁻¹) and BiVO₄ (0.00247 min⁻¹), respectively. It was observed that this composite is stable and it could retain around 90% of its initial photocatalytic activity even after four cycles.

Badvi and Javanbakht²⁴ prepared ZSM-5/TiO₂ nanophotocatalysts by dispersing TiO₂ onto the surface of the ZSM-5 zeolite via sole-gel method. It was followed by calcination at different temperatures and finally modified with different amounts of nickel nanoparticles.

Its activity for degradation of methylene blue was observed under UV light irradiation and it was compared with other methods such as catalytic hydrogen peroxide oxidation, hydrogen peroxide-assisted photocatalytic degradation and adsorption processes. It was reported that highest UV photocatalytic degradation efficiency of MB could be obtained as 99.80% on using 0.5% nickel nanoparticle calcined at 600 °C.

Kumar et al.²⁵ prepared pristine copper and iron layered double hydroxide (LDH) doped with zirconium via coprecipitation method. Then they embedded it with reduced graphene oxide. As-prepared composite (ZrRGOCuFe LDHs) was used for photodegradation of methylene blue in aqueous solution. Here, pristine CuFe LDH was doped with Zr and RGO to afford better heterogeneous catalysts within ZrRGOCuFe LDH dopants and band gap was obtained between 1.74 and 2.0 eV.

It was revealed that higher photodegradation efficiency of 95.2% could be achieved using this photocatalyst within 75 min at pH 7, photocatalyst dosage (1.0 g L^{-1}) and methylene blue (10 ppm) under visible light irradiation. It was also observed that 92% total organic content was removed. The catalyst has stability and reusability even after three successive cycles.

Peerakiatkhajohn et al.²⁶ synthesized ZnO and aluminum doped ZnO nanoparticles (Al/ZnO NPs) through sol-gel method at calcination temperatures (200, 300 and 400° C) and different Al dosage (1, 3, 5 and 10%). It was observed that structure of ZnO NPs were spherical, nanorod and nanoflake for calcination temperatures at 200, 300 and 400° C, respectively. It was also revealed that ZnO NPs calcined at 200° C exhibited higher removal efficiency of methylene orange (80%) after 4 h under the UV light irradiation, due to more light absorption property and highest specific surface area, while 5% Al/ZnO samples displayed 99% removal efficiency in only 40 min, which was almost 20 times higher in photocatalytic activity as compared to pristine ZnO under visible light irradiation.

Qutub et al.²⁷ prepared cadmium sulphide nanostructures doped with titanium oxide (CdS/TiO₂) nanocomposites via a modified chemical precipitation method. The photocatalytic efficiency of TiO₂/CdS nanocomposites was evaluated in the visible region. It was observed that as-prepared CdS-TiO₂ nanocomposites exhibited the highest photocatalytic activity (84%) in photocatalytic degradation of acid blue 29 (AB-29), while CdS and TiO₂ showed only 68 and 09% after 1 h and 30 min of visible light irradiation, respectively. This increased photocatalytic effectiveness of CdS-TiO₂ has been attributed to reduced charge carrier recombination and extension of TiO₂ in response to visible light.

Almehizia et al.²⁸ prepared ZnO nanoparticles via combustion method using L-alanine, L-arginine and L-valine as organic fuels. It was reported that average crystallite size of these samples was 25.24, 31.11, and 35.65 nm on using L-arginine, L-valine, and L-alanine fuels, respectively. It was observed that these ZnO samples were of irregular, hexagonal, and spherical shapes respectively. The band gap of these ZnO samples was found to be 3.30, 2.88, and 2.63 eV, respectively. It was also revealed that these samples could degrade 50 mL of methylene blue (10 mg L^{-1}) dye under UV irradiations by 54.69, 41.34, and 30.76% in one and half h, respectively, however, it reached to 100% in presence of hydrogen peroxide within 70 min in case of L-arginine as fuel.

Verma et al.²⁹ synthesized titanium dioxide nanoparticles (TiO₂ NPs) and titanium dioxide-graphene oxide (T/G) nanocomposites. They used both; TiO₂NPs and T/G nanocomposites for photocatalytic degradation of methylene blue and malachite green. It was reported that 85 and 93 % of malachite green and methylene blue could be degraded in 13 and 60 min, respectively under visible light irradiation.

Wang et al.³⁰ constructed Z-scheme AgI/Sb₂WO₆ heterojunction via a chemical-precipitation method. It was used for photocatalytic degradation of rhodamine B and tetracycline under visible light illumination. It was reported that about 95 and 80% degradation could be achieved in 12 and 8 min, which is 10.8 and 11.4 times higher with Sb₂WO₆, alone respectively.

Hwang et al.³¹ synthesized a multifunctional photocatalyst via metal oxides loaded (Co/Pd) on acid-treated TiO₂ nanorods (ATO) and then introduced hydrogen via annealing treatment. It was observed that hydrogen-treated photocatalyst (Pd (1) Co (1)/ATO (red)) exhibited high degradation efficiencies of 99.63 and 99.90% for orange II and bisphenol A (BPA) degradation in 3 h respectively.

Pandeya et al.³² fabricated a series of splendid flexible CdS/TiO₂ (CdS/TZ) nanofibrous membranes (NFMs) and used for photocatalytic degradation of methyl orange. It was reported that degradation efficiency of CdS/TiO₂ was 96.8% in 1 h and photocatalyst retained its photocatalytic activity up to five consecutive cycles. It was also revealed that chemical oxygen demand (COD) removal efficiency for TiO₂ membrane alone was 74.16%, only, which was increased to 91.66% for composite CdS/TiO₂ membrane.

Masekela et al.³³ immobilized tri-component (Sb-ZnO/MoS₂) on fluorine-doped tin oxide (FTO). Then they used as-developed tri-component for catalytic degradation of methyl orange (MO), methylene blue (MB), and ciprofloxacin (CIP) under light and ultrasonic vibration. It was reported that coupling of light (photocatalysis) and ultrasonic irradiation (piezocatalysis) exhibited greater degradation efficiencies of 95, 82, and 72% for methylene blue, methylene orange, and ciprofloxacin, respectively. It was also revealed that degree of mineralization was 76, 70, and 52% for MB, MO, and CIP, respectively as evident from total organic carbon (TOC) analysis.

Qing et al.³⁴ prepared composite membranes using polyvinylidene fluoride (PVDF) as the substrate, polyvinylpyrrolidone (PVP) as the dispersing agent & wettability regulator and cuprous oxide as the photocatalyst. These membranes were used for photocatalytic degradation of methyl orange (MO), methylene blue (MB), and Congo red (CR). It was also revealed that higher photocatalytic degradation ratio for methyl orange (93.6%) was there. This as-prepared membrane also had excellent recycling stability, and it can retain its removal ability to 92.1% even after using it 5 times. It was reported that these composite membranes also displayed high removal ability of methylene blue (81.4) and (76.1%).

Advanced oxidation processes (AOPs) are emerging as a potential technology for the treatment of pollutant water. Out of these, photocatalysis plays a dominant role to degrade organic contaminants to almost harmless or less harmful products. It is also a green chemical pathway as it takes care of environment in advance.

15.5 References:

1. Ledakowicz, S., Solecka, M., and Zylla, R., Biodegradation, decolourisation and detoxification of textile wastewater enhanced by advanced oxidation processes, *J. Biotechnol.*, **2001**, 89(2-3), 175-184.
2. Tang, J., Zou, Z., Yin, J., and Ye, J., Photocatalytic degradation of methylene blue on CaIn_2O_4 under visible light irradiation, *Chem. Phys. Lett.*, **2003**, 382(1-2), 175-179
3. Liqiang, J., Baiqi, W., Baifu, X., Shudan, L., Keying, S., Weimin, C., et al., Investigations on the surface modification of ZnO nanoparticle photocatalyst by depositing Pd, *J. Solid State Chem.*, **2004**, 177(11), 4221-4227.
4. Chen, F., Zou, W., Qu, W., and Zhang, J., Photocatalytic performance of a visible light TiO_2 photocatalyst prepared by a surface chemical modification process, *Catal. Commun.*, **2009**, 10(11), 1510-1513.
5. Wu, Y., Xing, M., Zhang, J., and Chen, F., Effective visible light-active boron and carbon modified TiO_2 photocatalyst for degradation of organic pollutant, *Appl. Catal. B: Environ.*, **2010**, 97(1-2), 182-189.
6. Pan, C., and Zhu, Y., New type of BiPO_4 oxy-acid salt photocatalyst with high photocatalytic activity on degradation of dye, *Environ. Sci. Technol.*, **2010**, 44(14), 5570-5574.
7. Yu, H., Xu, L., Wang, P., Wang, X., and Yu, J., Enhanced photoinduced stability and photocatalytic activity of AgBr photocatalyst by surface modification of Fe (III) cocatalyst, *Appl. Catal. B: Environ.*, **2014**, 144, 75-82.
8. Bai, X., Wang, L., Wang, Y., Yao, W., and Zhu, Y., Enhanced oxidation ability of g- C_3N_4 photocatalyst via C_{60} modification, *Appl. Catal. B: Environ.*, **2014**, 152, 262-270.
9. Tripathy, N., Ahmad, R., Song, J. E., Ko, H. A., Hahn, Y. B., and Khang, G., Photocatalytic degradation of methyl orange dye by ZnO nanoneedle under UV irradiation, *Mater. Lett.*, **2014**, 136, 171-174.
10. Balcha, A., Yadav, O. P., and Dey, T., Photocatalytic degradation of methylene blue dye by zinc oxide nanoparticles obtained from precipitation and sol-gel methods, *Environ. Sci. Pollut. Res.*, **2016**, 23, 25485-25493. doi.org/10.1007/s11356-016-7750-6.
11. Thi, V. H. T., and Lee, B. K., Effective photocatalytic degradation of paracetamol using La-doped ZnO photocatalyst under visible light irradiation, *Mater. Res. Bull.*, **2017**, 96, 171-182.
12. Sudrajat, H., and Babel, S., A novel visible light active N-doped ZnO for photocatalytic degradation of dyes, *J. Water Process. Eng.*, **2017**, 16, 309-318.
13. Wu, Y., Wang, H., Tu, W., Liu, Y., Tan, Y. Z., Yuan, X., et al., Quasi-polymeric construction of stable perovskite-type $\text{LaFeO}_3/\text{g-C}_3\text{N}_4$ heterostructured photocatalyst for improved Z-scheme photocatalytic activity via solid pn heterojunction interfacial effect, *J. Hazard. Mater.*, **2018**, 347, 412-422.
14. Huang, S., Chen, C., Tsai, H., Shaya, J., and Lu, C., Photocatalytic degradation of thiobencarb by a visible light-driven MoS_2 photocatalyst, *Sep. Purif. Technol.*, **2018**, 197, 147-155.
15. Jiang, L., Yuan, X., Zeng, G., Wu, Z., Liang, J., Chen, X., et al., Metal-free efficient photocatalyst for stable visible-light photocatalytic degradation of refractory pollutant, *Appl. Catal. B: Environ.*, **2018**, 221, 715-725.
16. Lu, C., Guo, F., Yan, Q., Zhang, Z., Li, D., Wang, L., et al., Hydrothermal synthesis of type II $\text{ZnIn}_2\text{S}_4/\text{BiPO}_4$ heterojunction photocatalyst with dandelion-like microflower

- structure for enhanced photocatalytic degradation of tetracycline under simulated solar light, *J. Alloys Compd.*, **2019**, 811, doi.org/10.1016/j.jallcom.2019.151976.
17. Mahanthappa, M., Kottam, N., and Yellappa, S., Enhanced photocatalytic degradation of methylene blue dye using CuSCdS nanocomposite under visible light irradiation, *Appl. Surf. Sci.*, **2019**, 475, 828-838. doi.org/10.1016/j.apsusc.2018.12.178.
 18. Tichapondwa, S. M., Newman, J. P., and Kubheka, O., Effect of TiO₂ phase on the photocatalytic degradation of methylene blue dye, *Phys. Chem. Earth., Parts A/B/C*, **2020**, 118, doi.org/10.1016/j.pce.2020.102900.
 19. Kiwaan, H. A., Atwee, T. M., Azab, E. A., and El-Bindary, A. A., Photocatalytic degradation of organic dyes in the presence of nanostructured titanium dioxide, *J. Mol. Struct.*, **2020**, 1200, doi.org/10.1016/j.molstruc.2019.127115.
 20. Tripathi, R. M., Hameed, P., Rao, R. P., Shrivastava, N., Mittal, J., and Mohapatra, S., Biosynthesis of highly stable fluorescent selenium nanoparticles and the evaluation of their photocatalytic degradation of dye, *Bionanosci.*, **2020**, 10, 389-396.
 21. Aziz, A., Ali, N., Khan, A., Bilal, M., Malik, S., Ali, N., and Khan, H., Chitosan-zinc sulfide nanoparticles, characterization and their photocatalytic degradation efficiency for azo dyes, *Int. J. Biol. Macromol.*, **2020**, 153, 502-512. doi.org/10.1016/j.ijbiomac.2020.02.310
 22. Uheida, A., Mejía, H. G., Abdel-Rehim, M., Hamd, W., and Dutta, J., Visible light photocatalytic degradation of polypropylene microplastics in a continuous water flow system, *J. Hazard. Mater.*, **2021**, 406, doi.org/10.1016/j.jhazmat.2020.124299.
 23. Liu, L., Hu, T., Dai, K., Zhang, J., and Liang, C., A novel step-scheme BiVO₄/Ag₃VO₄ photocatalyst for enhanced photocatalytic degradation activity under visible light irradiation, *Chinese J. Catal.*, **2021**, 42(1), 46-55.
 24. Badvi, K., and Javanbakht, V., Enhanced photocatalytic degradation of dye contaminants with TiO₂ immobilized on ZSM-5 zeolite modified with nickel nanoparticles, *J. Clean. Prod.*, **2021**, 280, doi.org/10.1016/j.jclepro.2020.124518.
 25. Kumar, O. P., Ashiq, M. N., Shah, S. S. A., Akhtar, S., Obaidi, M. A. A., Mujtaba, et al., Nanoscale ZrRGOCuFe layered double hydroxide composites for enhanced photocatalytic degradation of dye contaminant, *Mater. Sci. Semicond. Process.*, **2021**, 128, doi.org/10.1016/j.mssp.2021.105748.
 26. Peerakiatkhajohn, P., Butburee, T., Sul, J. H., Thaweesak, S., and Yun, J. H., Efficient and rapid photocatalytic degradation of methyl orange dye using Al/ZnO nanoparticles, *Nanomater.*, **2021**, 11(4), doi.org/10.3390/nano11041059.
 27. Qutub, N., Singh, P., Sabir, S., Sagadevan, S., and Oh, W. C., Enhanced photocatalytic degradation of acid blue dye using CdS/TiO₂ nanocomposite, *Sci. Rep.*, **2022**, 12(1), doi: 10.1038/s41598-022-09479-0.
 28. Almehizia, A. A., Al-Omar, M. A., Naglah, A. M., Bhat, M. A., and Al-Shakliah, N. S., Facile synthesis and characterization of ZnO nanoparticles for studying their biological activities and photocatalytic degradation properties toward methylene blue dye, *Alex. Eng. J.*, **2022**, 61(3), 2386-2395. doi.org/10.1016/j.aej.2021.06.102.
 29. Verma, N., Chundawat, T. S., Chandra, H., and Vaya, D., An efficient time reductive photocatalytic degradation of carcinogenic dyes by TiO₂-GO nanocomposite, *Mater. Res. Bull.*, **2023**, 158, doi.org/10.1016/j.materresbull. 2022.112043.
 30. Z. Wang, W. Li, J. Wang, Y. Li, G. Zhang, Novel Z-scheme AgI/Sb₂WO₆ heterostructure for efficient photocatalytic degradation of organic pollutants under

- visible light: Interfacial electron transfer pathway, DFT calculation and mechanism unveiling, *Chemosphere*, **311**, **2023**
doi.org/10.1016/j.chemosphere.2022.137000
31. I. S. Hwang, V. Manikandan, R. P. Patil, M. A. Mahadik, W.-S. Chae, H.-S. Chung, S. H. Choi, and J. S. Jang, Hydrogen-treated TiO₂ nanorods decorated with bimetallic Pd–Co nanoparticles for photocatalytic degradation of organic pollutants and bacterial inactivation, *ACS Appl. Nano Mater.* **2023** **6** (3), 1562-1572
 32. doi: 10.1021/acsanm.2c04160
 33. S. Pandeya, R. Ding, Y. Ma, X. Han, M. Gui, P. Mulmi, K. P. Panthi, B. B. Neupane, H. R. Pant, Z. Li, M. K. Joshi, Self-standing CdS/TiO₂ Janus nanofibrous membrane: COD removal, antibacterial activity and photocatalytic degradation of organic pollutants, *J. Environ. Chem. Eng.*, **12**(3), **2024** doi.org/10.1016/j.jece.2024.112521
 34. D. Masekela, N. C. Hintsho-Mbita, L. N. Dlamini, T. L. Yusuf, N. Mabuba, Internal piezoelectric field produced by tri-component (FTO: Sb-ZnO/MoS₂) thin film for enhanced photocatalytic degradation of organic pollutants and antibacterial activity, *Mater. Today Commun.*, **38**, **2024** doi.org/10.1016/j.mtcomm.2024.108500
 35. Q. Qing, S.-Y. Chen, S.-Z. Hu, L. Li, T. Huang, N. Zhang, and Y. Wang, highly efficient photocatalytic degradation of organic pollutants using a polyvinylidene fluoride/polyvinylpyrrolidone-cuprous oxide composite membrane, *Langmuir* **2024** **40** (2), 1447-1460, doi: 10.1021/acs.langmuir.3c03168